

# Asymmetry distributions and mass effects in dijet events at a polarized HERA <sup>1</sup>

M. Maul <sup>a</sup>, A. Schäfer <sup>a</sup>, E. Mirkes <sup>b</sup>, and G. Rädcl <sup>c</sup>

<sup>a</sup> *Institute for Theoretical Physics, 93040 Regensburg, Germany.*

<sup>b</sup> *Institute for Theoretical Particle Physics, 76128 Karlsruhe, Germany.*

<sup>c</sup> *CERN - Div. PPE, 1211 Genève 23, Switzerland.*

The asymmetry distributions for several kinematic variables are considered for finding a systematic way to maximize the signal for the extraction of the polarized gluon density. The relevance of mass effects for the corresponding dijet cross section is discussed and the different approximations for including mass effects are compared. We also compare via the programs PEPSI and MEPJET two different Monte Carlo (MC) approaches for simulating the expected signal in the dijet asymmetry at a polarized HERA.

PACS: 13.60.Hb,13.85.Hd,12.40.Ee

Keywords: deep inelastic scattering, semi inclusive mass effects, angle distribution

---

<sup>1</sup>Work supported in part by BMBF

# 1 Introduction

The isolation and investigation of the polarized gluon parton distribution is one of the most interesting topics for deep inelastic scattering. The three main approaches are the analysis of dijet events, on which we will concentrate here, the  $Q^2$  dependence of structure functions [1], and the production of charmed particles [2]. Up-to-date parton distributions based on all experimental input available do not yet determine the form of the polarized gluon distribution with any degree of reliability [3]. This underscores the great significance of a polarized HERA, where all three approaches described above would be feasible.

In the analysis of dijet events two different processes have to be taken into account, the photon-gluon fusion (PGF) and the gluon bremsstrahlung (GB), see Fig. 1. Only the photon-gluon fusion allows to analyze the gluon parton distribution, while the gluon bremsstrahlung is a background process. In the following we will investigate to which extent we can get information about the PGF events from the polarized dijet cross section. For this purpose we discuss in the first section, after some remarks to the kinematic cuts used, the influence of quark and remnant masses on the dijet cross section in different MC approaches. In the second section we analyze the spin asymmetry of dijet events as a function of several kinematic variables. We present a method of how to find suitable cuts in these kinematic variables so that the significance of the asymmetry signal becomes largest. This is a continuation of the discussion started in [4], where the discussion was concentrated on the kinematic variable  $x_g$ , the fractional momentum carried by the gluon.

The discussion is done on the level of parton jets because on this level the QCD improved parton model provides a well defined theory, where comparison of different MC approaches is possible in a quantitative way. Moreover, this will be the bases for more parameter-dependent additions like parton showering, to describe higher-order effects, and fragmentation. We should stress, however, that the advances in jet reconstruction justify a discussion on this level. For the simulations we use the following two MC generators PEPSI and MEPJET. PEPSI is a polarized add-on package to the unpolarized LEPTO-6.5 code. The general principles are the same as in the earlier version PEPSI 1 [6]. The code contains massless partonic cross sections, where the effects of heavy quark masses and remnant target masses are taken into account by constraints reflecting energy-momentum conservation of massive particles.

As to the MEPJET code [7] we will here use two versions. The first one neglects quark and target remnant masses, even charm and bottom quarks are treated as massless. The second one contains the quark masses in the photon-gluon fusion cross section, but neglects the influence of the target remnant mass. We use this fact to demonstrate the quark and remnant mass threshold effects in our simulations by comparing the PEPSI with the MEPJET results. We show that those effects are small for QCD bremsstrahlung

and large for photon-gluon fusion.

## 2 Mass effects and kinematics

The calculations are done for HERA energies, i.e., 820 GeV protons are scattered off 27.5 GeV electrons. The cuts used are compatible with the present detectors at HERA. The option of polarized protons is discussed as a possible HERA upgrade [4]. We use the following maximal kinematic cuts:

$$\begin{aligned} 10^{-5} &< x < 1 \\ 0.3 &< y < 0.8 \\ 5 \text{ GeV}^2 &< Q^2 < 100 \text{ GeV}^2 \quad . \end{aligned} \tag{1}$$

$Q^2 = -q^2$  is the virtuality of the photon,  $x = Q^2/(2P \cdot q)$  the usual Bjorken  $x$ ,  $y = (P \cdot q)/(P \cdot k)$ , and  $k$  the momentum of the incoming lepton. The cut in  $Q^2$  is guided by the idea that we look for such a kinematic range, where the fusion process is by far dominating the bremsstrahlung process (see also [4]). This is, of course an indirect effect because the low  $Q^2$  implies small  $x$ , which in principle accounts for the large gluon contribution. The cut  $y > 0.3$  does not originate from detector requirements, but is due to the fact that the spin-dependent part of the cross section, which is proportional to  $y(1 - y/2)$ , becomes small for small  $y$ . The very point is that it is not possible with totally inclusive methods to single out the photon-gluon fusion contribution. This would be possible by triggering on charm or bottom quarks, but those particles can only be detected indirectly, which is connected to losses in statistics. So, by combining both methods one can get a quite reliable method of extracting  $\Delta G$  from DIS data. For the detection of the jets we use an algorithm which may be called a combined  $z$ - $s$ -cone scheme [Eq. (3)]. This is done in order to be able to work in the same jet scheme in PEPSI/LEPTO and MEPJET because in this point the two codes differ substantially. The following parameters are set:

$$\begin{aligned} z_{\min} &= 0.04 \\ \hat{s}_{\min} &= 100 \text{ GeV}^2 && \text{PEPSI} \\ s_{ij,\min} &= 100 \text{ GeV}^2 && \text{PEPSI, MEPJET} \\ R_{\min} &= 1.0 \\ p_{T\min} &= 5 \text{ GeV} \quad . \end{aligned} \tag{2}$$

$z_{\min}$  is the minimum of  $z = (P \cdot p_{\text{jet}})/(P \cdot q)$  for the two jet four-momenta  $p_{\text{jet}}$  in a dijet event. The value  $z_{\min} = 0.04$  is the default value of LEPTO-6.5.  $\hat{s}_{\min}$  is defined via  $\hat{s} := (p + q)^2$ , where  $p$  is the four-momentum of the incoming quark. The  $\hat{s}$  cut is ineffective due to the large  $p_T$  cut. We furthermore require for the invariant mass of the two jets  $s_{ij} := (p_1 + p_2)^2 > 100 \text{ (GeV)}^2$ , where  $p_1$  and  $p_2$  are the two jet four-momenta. It has to be noticed that the cuts in  $Q^2$  and  $p_T$  are the smallest values possible in order to get reliable results within the LO cross sections. For smaller values NLO effects become dominant and the LO simulations are no longer applicable in a reliable way.  $R_{\min}$  defines

the minimal cone distance which two partons must have in order to belong to different jets. The cone distance is given by the Pythagorean sum of azimuthal deviation  $\Delta\phi$  and pseudo rapidity difference  $\Delta\eta$ , i.e.:

$$R = \sqrt{(\Delta\eta)^2 + (\Delta\phi)^2} \quad . \quad (3)$$

Finally, for  $\alpha_S$  we use the one-loop expression with  $\Lambda_{\text{QCD}} = 151$  MeV (which is the value for  $\Lambda_{\text{QCD}}$  over the bottom threshold), i.e.:

$$\alpha_S(Q^2) = \frac{4\pi}{(11 - \frac{2}{3}n_f) \ln(Q^2/\Lambda_{\text{QCD}}^2)} \quad . \quad (4)$$

For  $\alpha_{\text{em}}$  we use the standard form as implemented in JETSET [9]. For the interesting asymmetries, i.e., the ratio of the polarized and the unpolarized cross section, these coupling constants will cancel out. Regarding the parton distributions, we use the set 'Gluon A' from Gehrmann and Stirling [10] as the polarized one and the 'GRV leading order (LO) set' given in [12] as the unpolarized one. For the observables discussed here we have checked that the qualitative behavior is the same for the standard LO scenario discussed in [11]. The influence of several different models of  $\Delta G$  on the polarized dijet cross section has been discussed in [4].

We first focus on the angle  $\Theta$  between the spatial momenta of the exchanged photon and the outgoing quark jet. From a theoretical point of view we can define an angle  $\Theta^{\text{th}}$  as the angle between the exchanged photon and the outgoing quark jet in the cm system of the two outgoing jets. Then, in Fig. 2 the upward going jet 1 would be a quark jet and the downward going jet 2 would be an anti-quark jet or a gluon jet. Such a definition, although interesting for theoretical considerations, is not accessible experimentally because one cannot distinguish between quark, anti-quark and gluon jets. An experimentally accessible definition ( $\Theta^{\text{exp}}$ ) would be that  $\Theta^{\text{exp}}$  is the intersection angle (smaller than 90 degrees) between the line formed by the two jets in their cm system and the incoming photon.  $\Theta^{\text{th}}$  is connected with the variable  $z$  from Eq. (2) via the relation  $z = \cos^2(\Theta^{\text{th}}/2)$ . In order to isolate the pure spin-dependent contribution one first regards the cross sections for anti-parallel ( $d\sigma(\uparrow\downarrow)$ ) and parallel spins ( $d\sigma(\uparrow\uparrow)$ ) of the colliding proton and electron beams. One then takes the mean and half of the difference of the differential cross sections of the two polarization configurations:

$$\begin{aligned} d\sigma &= \frac{1}{2}(d\sigma(\uparrow\downarrow) + d\sigma(\uparrow\uparrow)) \quad , \\ d\Delta\sigma &= \frac{1}{2}(d\sigma(\uparrow\downarrow) - d\sigma(\uparrow\uparrow)) \quad . \end{aligned} \quad (5)$$

In Fig. 3 we compare the polarized and unpolarized  $\Theta^{\text{th}}$  distributions and the predicted asymmetries as calculated with PEPSI (filled squares) and MEPJET (histogram). The large deviations for the photon-gluon fusion cross sections are due to the treatment of the quark masses and target remnant masses. For the shown MEPJET results quark masses

and target remnant masses are neglected completely. In PEPSI/LEPTO they are taken into account via threshold effects only, i.e., the energy and momentum must be fulfilled when the quark masses and remnant masses are added to the jet four-vectors, whereas the cross sections in PEPSI/LEPTO are calculated for massless partons. As Fig. 3 shows, both effects are nearly absent for the gluon-bremsstrahlung process, while they play a crucial role for the photon-gluon fusion. Moreover, the effect due to the target remnant mass is dominating. Effectively this remnant mass is included into the LEPTO code in such a way that not only the massive quark anti-quark pair, but also the remnant has to be generated from the momentum four-vectors of the incoming photon and proton. In the case of the gluon bremsstrahlung such an effect is absent because as gluons are massless there is effectively no energy necessary to radiate a gluon.

To demonstrate this we take an upgraded version of MEPJET, which takes into account the exact cross section for photon gluon fusion with quark masses and compare this to a PEPSI run where we substitute the target remnant by a simple massless gluon (see Tab. 1). In all cases we take the heavy quark masses to be  $m_c = 1.35$  GeV and  $m_b = 5$  GeV, as used in standard JETSET. The two cross sections are qualitatively in agreement. Note that they may not agree exactly because PEPSI/LEPTO takes quark masses into account only via threshold constraints, i.e., energy-momentum constraints inserted into massless cross sections, while MEPJET in the unpolarized case takes quark masses exactly into account. Unfortunately, there is so far no polarized version of the massive MEPJET available. Besides, as the agreement shows, the PEPSI/LEPTO implementation of quark masses is a quantitatively good approximation to the exact quark mass treatment, and, moreover, the absolute effect of the quark masses in the final state is only about 5-6% of the total cross section. When taking into account also the mass of the remnant, the photon-gluon fusion cross section is reduced by another 10%. There is no corresponding reduction in the bremsstrahlung cross section. This is due to the fact that for emitting a gluon, which is massless by itself, the energy can be in principle arbitrarily small.

Moreover, the quark mass effects, as implemented in PEPSI enter the polarized and the unpolarized cross sections in the same way. For the asymmetries, displayed in the last row of Fig. 3, the agreement between the two programs is consequently nearly exact. This on the other hand means that for asymmetry calculations we can use the massless program to get proper results. The numbers for the total cross sections are given in Tab. 1 for the unpolarized case and in Tab. 2 for the polarized case. The errors are the statistical MC errors, an inclusion of the systematic errors from parton distribution uncertainties etc. cannot be done in a reliable way. But taking the precision of present data as used in [10] for example, one could accept a systematic error of at least 10% to be realistic.

	cross sect. [ $pb$ ] GB event	cross sect. [ $pb$ ] PGF-event
MEPJET(1) massless version	$204.1 \pm 0.8$	$1057.6 \pm 3.3$
MEPJET(2) exact quark masses	$205.8 \pm 1.1$	$991.5 \pm 2.5$
PEPSI/LEPTO(1) approx. quark masses	$206.4 \pm 3.0$	$980.4 \pm 13.8$
PEPSI/LEPTO(2) approx. quark and remnant masses	$205.5 \pm 3.0$	$897.0 \pm 12.7$

Table 1: Treatment of quark masses in PEPSI/LEPTO and MEPJET in the unpolarized case.

### 3 Asymmetry distributions and optimization of kinematic cuts

Fig. 3 shows that the asymmetry is largest for angles  $\Theta^{\text{th}}$ , where the axis formed by the two jets lies close to the spatial momentum of the incoming photon, and that the quark jets in the gluon bremsstrahlung are accumulated slightly for the unpolarized case and distinctly for the polarized case close to the incoming photon. This has quite a natural reason as the quark jet in gluon bremsstrahlung is ordinarily more energetic than the respective gluon jet.

In Tab. 2 we give the integrated polarized cross sections. One should note again that the differences for the photon-gluon fusion come from the fact that in MEPJET quark masses are neglected. For a detailed discussion of the influence of quark masses on two and three jet rates see [8] and references therein. The most important question is how the significance of the asymmetry  $A = \frac{\Delta\sigma}{\sigma}$  can be amplified by suitable cuts. We will discuss several kinematic variables in the following. Let us first concentrate on the angle  $\Theta^{\text{exp}}$ . As there is no possibility to distinguish with 100% reliability quark- and gluon jets, only the angle between the axis formed by the dijet in its cm frame and the incoming photon in the same frame  $\Theta^{\text{exp}}$  is experimentally accessible. Of course then the asymmetry is large for small  $\Theta^{\text{exp}}$ , which can be already deduced from Fig. 3, but on the other hand a cut  $\Theta_{\text{max}}^{\text{exp}}$  also means losses in statistics. To get some feeling whether the signal could be improved, when imposing a  $\Theta_{\text{max}}^{\text{exp}}$  cut, we define the *significance sc* by the negative logarithm to the basis ten of the relative error in the asymmetry  $A$ .

	cross sect. [pb] PEPSI(2)	cross sect. [pb] MEPJET(1)
$\Delta$ GB-event	$3.80 \pm 0.12$	$3.93 \pm 0.02$
$\Delta$ PGF-event	$-37.71 \pm 0.63$	$-43.47 \pm 0.15$

Table 2: Polarized cross sections ( $\Delta\sigma$ ) for the kinematic used in the paper, comparing PEPSI(2) and the MEPJET(1) program.

(The choice of the basis ten is made to simplify rescaling for different luminosities.)

$$sc := -\log_{10}(\delta A/A) \quad . \quad (6)$$

Moreover, the logarithmic representation has the advantage to make it easier to plot large numerical ranges for  $\delta A/A$ . As the asymmetry is small for our kinematics, one can derive an approximative formula for the quadratic error of the asymmetry with only the luminosity and the unpolarized cross section:

$$\delta A = 2\sqrt{\frac{N_{\uparrow\uparrow} \cdot N_{\uparrow\downarrow}}{(N_{\uparrow\uparrow} + N_{\uparrow\downarrow})^3}} \approx \frac{1}{\sqrt{2L[\text{pb}^{-1}]\sigma_{\text{unpol}}}} \quad . \quad (7)$$

We can eliminate the luminosity from the significance formula by defining the reduced significance  $scr$ :

$$\begin{aligned} sc &:= -\log_{10}\left(\frac{2}{PA}\sqrt{\frac{\sigma_{\uparrow\uparrow} \cdot \sigma_{\uparrow\downarrow}}{(\sigma_{\uparrow\uparrow} + \sigma_{\uparrow\downarrow})^3}}\right) \\ &\quad + \frac{1}{2}\log_{10}(L[\text{pb}^{-1}]) \\ &=: scr + \frac{1}{2}\log_{10}(P^2L[\text{pb}^{-1}]) \quad . \end{aligned} \quad (8)$$

Here  $P = P_e P_p$  is the degree of polarization, which is the product of the degree of polarization of the proton beam  $P_p$  and the electron beam  $P_e$ , to include the effect of beam polarizations different from 100%. In this case the asymmetry is reduced while the absolute error, which depends approximately only on the unpolarized cross section, remains constant. In the following, if not something else is stated explicitly, the asymmetry plots will correspond to a degree of polarization of 100%. The luminosity  $L[\text{pb}^{-1}]$  is given per relative polarization, i.e.,  $N_{\uparrow\uparrow} = L\sigma_{\uparrow\uparrow}$  and  $N_{\uparrow\downarrow} = L\sigma_{\uparrow\downarrow}$ . If  $sc$  is zero or even negative then the error is as large or even larger than the signal. For a realistic

experiment  $sc$  should at least yield a number of 0.6, then one can set four bins with a two sigma signal each. The definition of  $scr$  allows to find the optimal cut for a maximal significance by a look on a single diagram. It is just a very economical way of visualizing the optimal parameter without trying several MC runs. In the following we plot the asymmetries versus several variables together with the reduced significances  $scr$  for the corresponding minimal or maximal cuts. In order to demonstrate the usefulness of this concept we show in Fig. 4 the asymmetry and  $scr$  for the experimentally accessible  $\Theta^{\text{exp}}$  and  $z^{\text{exp}}$  region.  $z^{\text{exp}}$  is the minimum of the two  $z$  values that belong to the two jets in Fig. 2. Both variables are closely related to each other because the more energetic one of the two parton jets is as compared to the other, i.e., the smaller  $z^{\text{exp}}$  is, the closer this jet will be aligned to the incoming photon in the frame defined in Fig. 2, i.e., the smaller is the angle  $\Theta^{\text{exp}}$  ( $z^{\text{exp}} = \cos^2((180^\circ - \Theta^{\text{exp}})/2)$ ). The asymmetry over both variables is displayed in Fig. 4. In both cases, the gluon bremsstrahlung reduces the asymmetry signal coming from photon-gluon fusion alone because the spin-dependent contributions to both processes differ in sign. From the shape of the asymmetries (left column in Fig. 4) one could suspect that a suitable  $\Theta_{\text{max}}^{\text{exp}}$  or  $z_{\text{max}}^{\text{exp}}$  cut would increase the measurable asymmetry signal. However, the significance plots on the right show that this is not the case. The reason for this is that the spin-dependent contribution  $\Delta\sigma$  is small, at most ten percent of the unpolarized cross section, and therefore the error [see Eq. (7)] is approximately anti-proportional to the square root of the unpolarized cross section alone. With decreasing  $\Theta_{\text{max}}^{\text{exp}}$  or  $z_{\text{max}}^{\text{exp}}$ , as can be seen in Fig. 3, the unpolarized cross section is reduced and therefore the error increases, over-compensating the gain in the asymmetry signal. As an illustration Fig. 5 shows the expected experimental errors for a luminosity of  $L = 100 \text{ pb}^{-1}$  per relative polarization, i.e.,  $L = 200 \text{ pb}^{-1}$  in total. The assumed electron and proton polarization is 70% each. The asymmetry is sizable using realistic cuts for the HERA machine. The envisaged luminosity allows to extract a clear and distinct signal in five bins, for example. The first bin corresponds to  $\Theta_{\text{max}}^{\text{exp}} = 28^\circ$ . The reduced significance for this cut in Fig. 4 is  $scr = -0.2232$ . For  $L = 100 \text{ pb}^{-1}$  per relative polarization and a degree of polarization of  $P = 0.5$  this corresponds to a relative error of 0.334.

We now turn to the  $p_T$  distributions in the lab system, see Fig. 6, where the maximum and the minimum  $p_T$  of the two jets is plotted. For pure photon-gluon fusion, the asymmetry is growing for larger  $p_{T,max}$ . Taking into account gluon bremsstrahlung the asymmetry is not only reduced, but also decreases above  $p_{T,max} = 25 \text{ GeV}$ . The behavior for  $p_{T,min}$  is similar. Moreover, as a glance to the reduced significances shows the relative error is increasing for increasing  $p_T$  cuts so that we recommend to choose, in spite of the behavior of the asymmetries, the  $p_T$  cut not larger than  $5 \text{ (GeV)}^2$ .

The same is true for the variable  $y$ , see Fig. 7, where again by increasing the  $y_{min}$  cut one gains in asymmetry but loses significance. The only way to increase the significance is by choosing a definite minimal cut for the invariant dijet mass  $s_{ij}$ , which should be of the order  $s_{ij,min} = 250 \text{ GeV}^2$ . However, it was shown in [4] that for unpolarized



jet production it is advisable to choose  $s_{ij,\min} = 500 \text{ GeV}^2$  in order to minimize next to leading order effects. A corresponding analysis for the polarized case awaits the implementation of the polarized NLO cross sections into MEPJET. As can be seen in Fig. 7, the losses in statistics for such cuts are not considerable.

The last variable discussed here is  $Q$ . The asymmetry distribution is nearly constant as a function of  $Q$ , so this is a completely uninteresting variable for improving the significance. On the other hand, as we show below, a suitable cut in  $Q$  allows to change the ratio of photon-gluon events to gluon bremsstrahlung events. In Fig. 8 we show the ratio of the total asymmetry and the pure gluonic asymmetry. The influence of gluon bremsstrahlung on the asymmetry increases for smaller  $Q_{\min}^2$ . The significance is considerably larger for small values of  $Q_{\min}^2$ , so one may think of choosing  $Q_{\min}^2$  as small as  $Q_{\min}^2 = 5 \text{ GeV}^2$  in the envisaged HERA experiments for extracting the polarized gluon density.

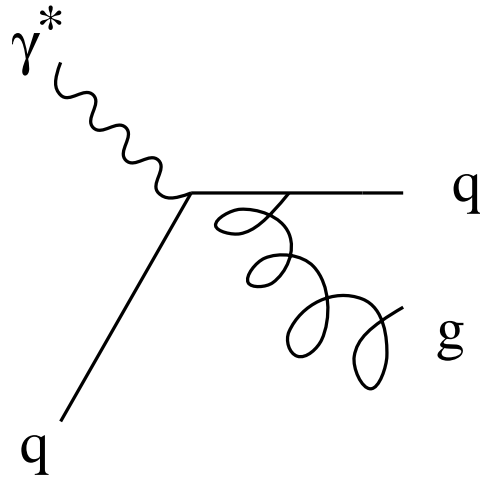
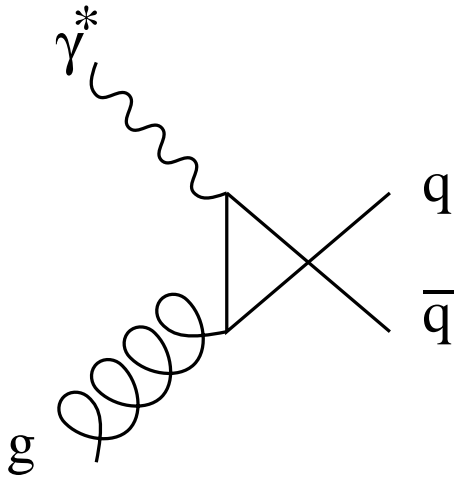
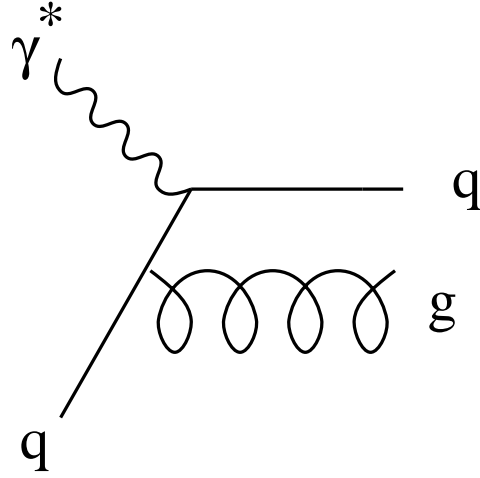
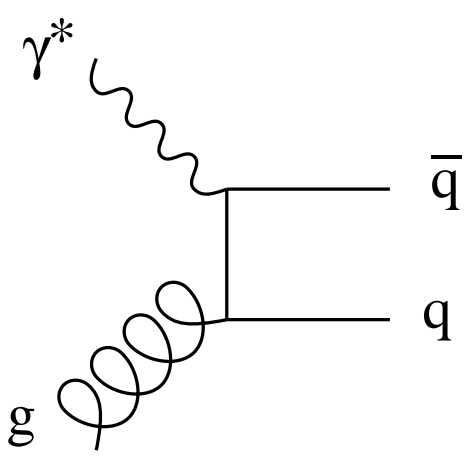
In summary we have found that the two programs PEPSI and MEPJET (in the massless version) agree for the predicted asymmetries, as the mass effects enter the polarized and unpolarized cross sections in PEPSI in the same way and therefore do not contribute to the asymmetry. For a polarized HERA the invariant dijet mass  $s_{ij,\min}$  plays a very special role, as it is the only variable where the significance of the dijet asymmetry signal can be slightly improved by increasing the minimal cut. For the invariant dijet mass one should choose an  $s_{ij,\min}$  cut between 250 and 500  $\text{GeV}^2$ . In all other cases studied here, it is advisable to choose small minimal cuts for  $\Theta^{\text{exp}}, z, p_T, y, Q^2$  in order to maximize the significance. However, the final choice of those cuts will be dictated by future studies comparing LO and NLO polarized calculations. We have shown that the influence of quark masses on the gluon bremsstrahlung cross section is negligible, while it is substantial for the photon-gluon fusion. A very dominant effect for the photon-gluon cross section may also arise from the remnant mass, which makes corrections on the 10% level. We have furthermore reproduced the observation that for a polarized HERA the asymmetry signal is sizable and highly significant for the envisaged luminosity of  $100 \text{ pb}^{-1}$  per relative polarization and 70% beam polarization.

**Acknowledgment:** The authors thank G. Ingelman, A. De Roeck, T. Gehrmann, and H. Ihssen for helpful discussions. M. M. and A. S. thank the BMBF, DESY and MPI für Kernphysik, Heidelberg for support.

## References

- [1] T. Gehrmann, W. J. Stirling Phys. Rev. D **53** (6100) 1996;  
M. Glück, E. Reya, M. Stratmann, W. Vogelsang, Phys. Rev. D **53** (4775) 1996.
- [2] A. D. Watson, Z. Phys. C **12** (123) 1982;  
G. Altarelli, W. J. Stirling, Part. World. **1** (40) 1989;

- M. Glück, E. Reya, W. Vogelsang Nucl. Phys. B **351** (579) 1991;  
T. Morii, S. Tanaka, T. Yamanishi Phys. Lett. B **322** (253) 1994;  
N. I. Kochelev, T. Morii, T. Yamanishi, Phys. Lett. B **405** (168) 1997.
- [3] S. Forte *Polarized structure functions: a status report*. DFTT-57-96, Oct 1996. 15pp. Invited talk at 14th International Conference on Particles and Nuclei (PANIC 96), Williamsburg, VA, 22-28 May 1996, and at 12th International Symposium on High-energy Spin Physics (SPIN96), Amsterdam, Netherlands, 10-14 Sep 1996. e-Print Archive: hep-ph/9610238.
- [4] A. De Roeck, J. Feltesse, F. Kunne, M. Maul, A. Schäfer, C.Y. Wu, E. Mirkes, G. Rädcl, *prospects for measuring  $\Delta G$  from jets at HERA with polarized protons and electrons* In \*Hamburg 1995/96, Future physics at HERA\* 803-814. e-Print Archive: hep-ph@xxx.lanl.gov - 9610315;  
J. Feltesse, F. Kunne, E. Mirkes, Phys. Lett. **B388** (1996) 832.
- [5] G. Ingelman, A. Edin, J. Rathsman, Comp. Phys. Commun. **101** (108) 1997.
- [6] L. Mankiewicz, A. Schäfer, M. Veltri, Comp. Phys. Commun. **71** (305) 1992.
- [7] E. Mirkes, D. Zeppenfeld, Phys. Lett. **B380** (1996) 205; The program can be obtained on request by the authors.
- [8] G. Vicente and R. Garcia, Oct. 1996. 95pp. Ph.D. Thesis. e-Print Archive: hep-ph@xxx.lanl.gov - 9703359.
- [9] T. Sjöstrand, Computer Physics Commun. **82** (1994) 74.
- [10] T. Gehrmann, W. J. Stirling, Phys. Rev. D **53** (6100) 1996.
- [11] M. Glück, E. Reya, M. Stratmann, W. Vogelsang, Phys. Rev. D **53** (4475) 1996.
- [12] M. Glück, E. Reya, A. Vogt, Z. Phys. C **67** (433) 1995.



photon-gluon fusion

gluon bremsstrahlung

**(PGF)**

**(BG)**

Figure 1: Feynmangraphs of photon-gluon fusion and gluon bremsstrahlung.

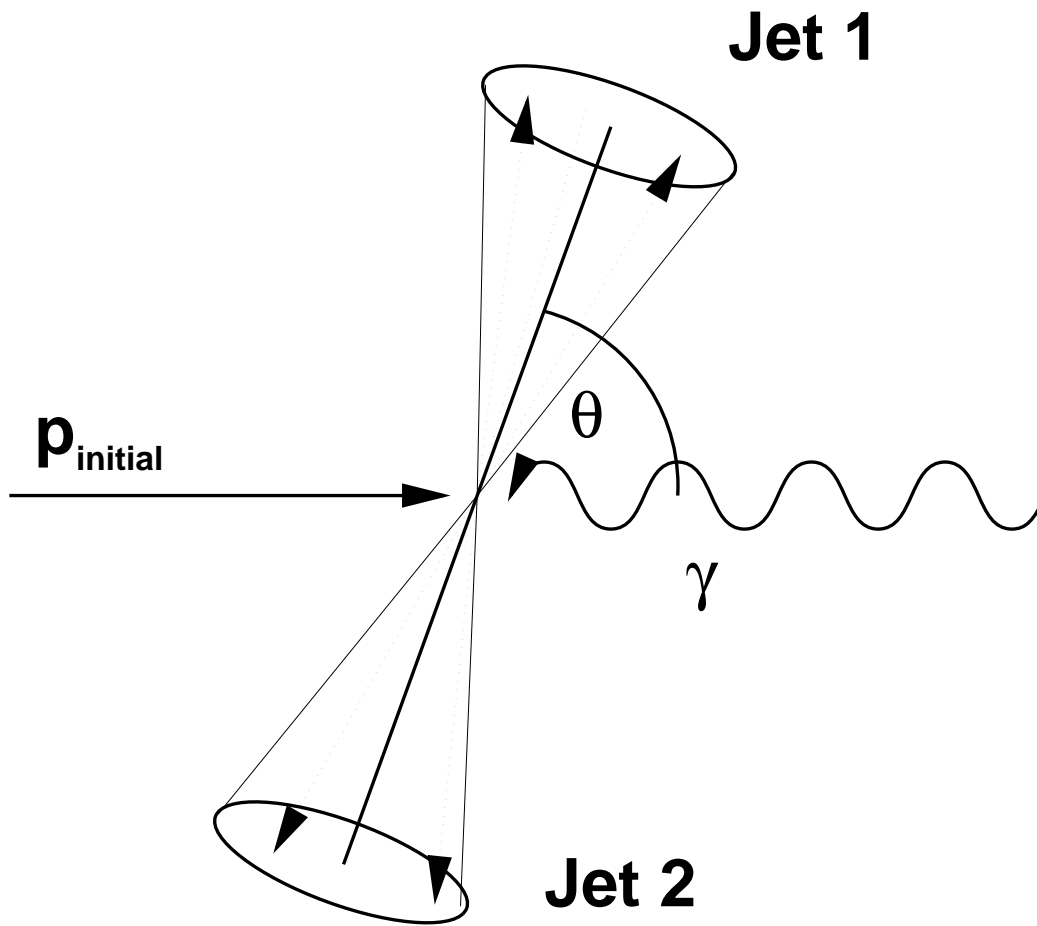


Figure 2: Definition of the angle  $\Theta$ : From a theoretical point of view an angle  $\Theta^{\text{th}}$  can be defined by the angle between the spatial momenta of the exchanged photon and the outgoing quark in the cm system of the two outgoing jets. Then the upward going jet 1 is a quark jet and the downward going an anti-quark or a gluon jet. But such a definition is not accessible experimentally because one cannot distinguish between quark, anti-quark and gluon jets. An experimental accessible definition ( $\Theta^{\text{exp}}$ ) is that  $\Theta^{\text{exp}}$  is the intersection angle (smaller than 90 degrees) between the line formed by the two jets in their cm system and the incoming photon line.

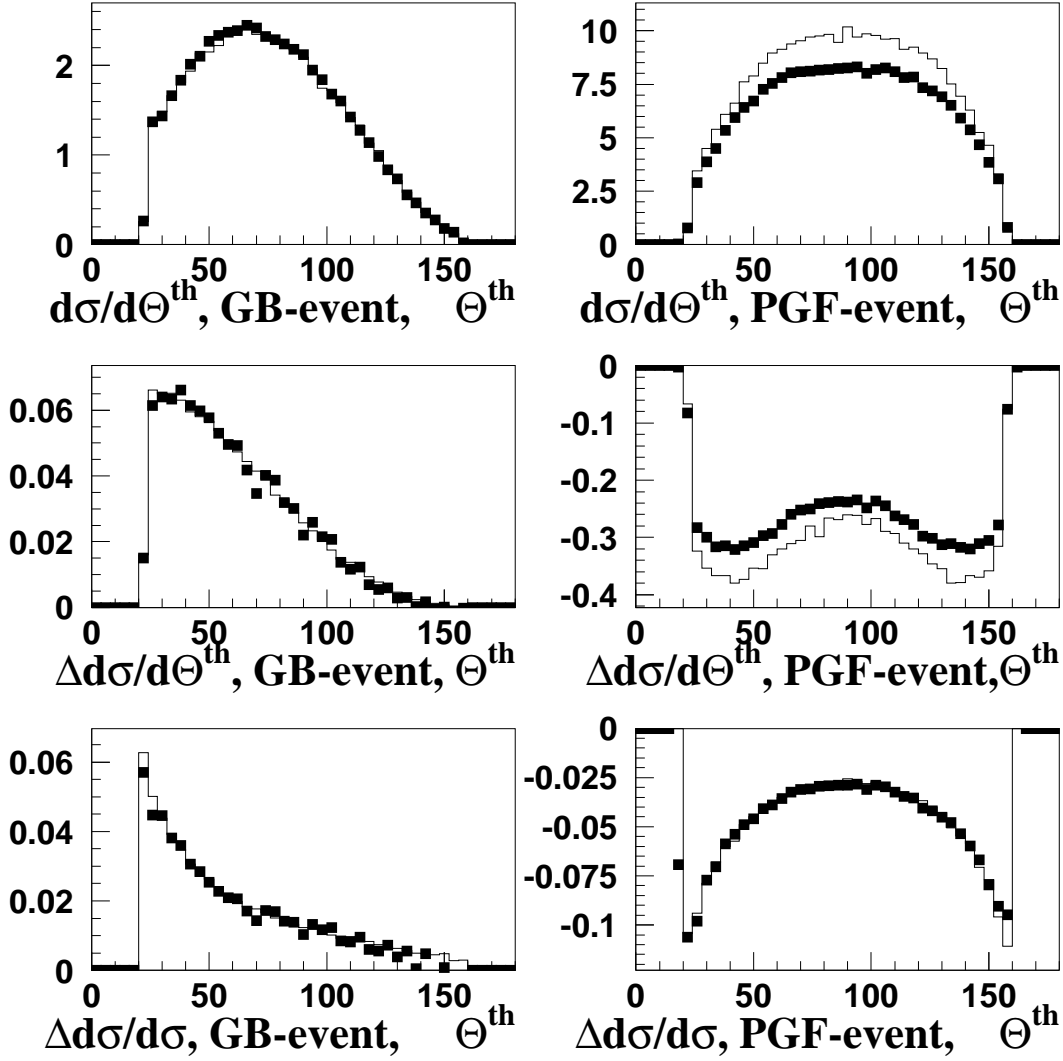


Figure 3: Influence of quark-mass effects to the unpolarized and polarized dijet cross sections. We show the results of the massless MEPJET program (histogram) and the PEPSI code (full squares), where quark-mass effects and remnant-mass effects are included. The units are in pb/degree.

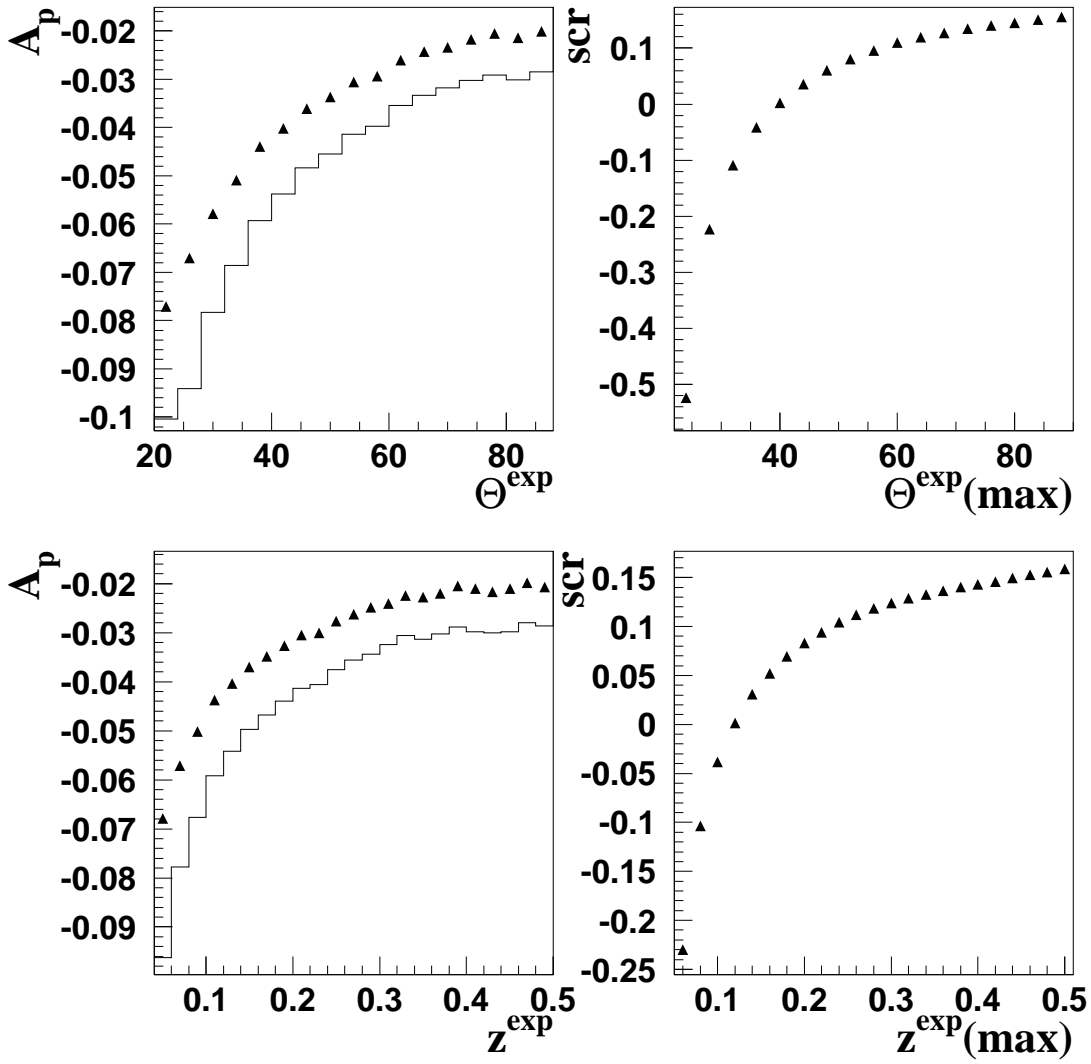


Figure 4: Asymmetry for proton beam  $A_p$  and reduced significance ( $scr$ ) for the  $\Theta^{\text{exp}}$ - and  $z^{\text{exp}}$  distributions. The histogram on the left hand side shows the asymmetry for photon-gluon fusion only. The triangles show the real asymmetry, which contains gluon bremsstrahlung as well as photon-gluon fusion. The pictures on the right show the significance ( $scr$ ) plotted against the  $\Theta_{\text{max}}^{\text{exp}}$  cut and  $z_{\text{max}}^{\text{exp}}$  cut, respectively. The data are simulated with PEPSI.

$\Theta^{\text{exp}}$ -dependence for  $L_p = 100 \text{ pb}^{-1}$

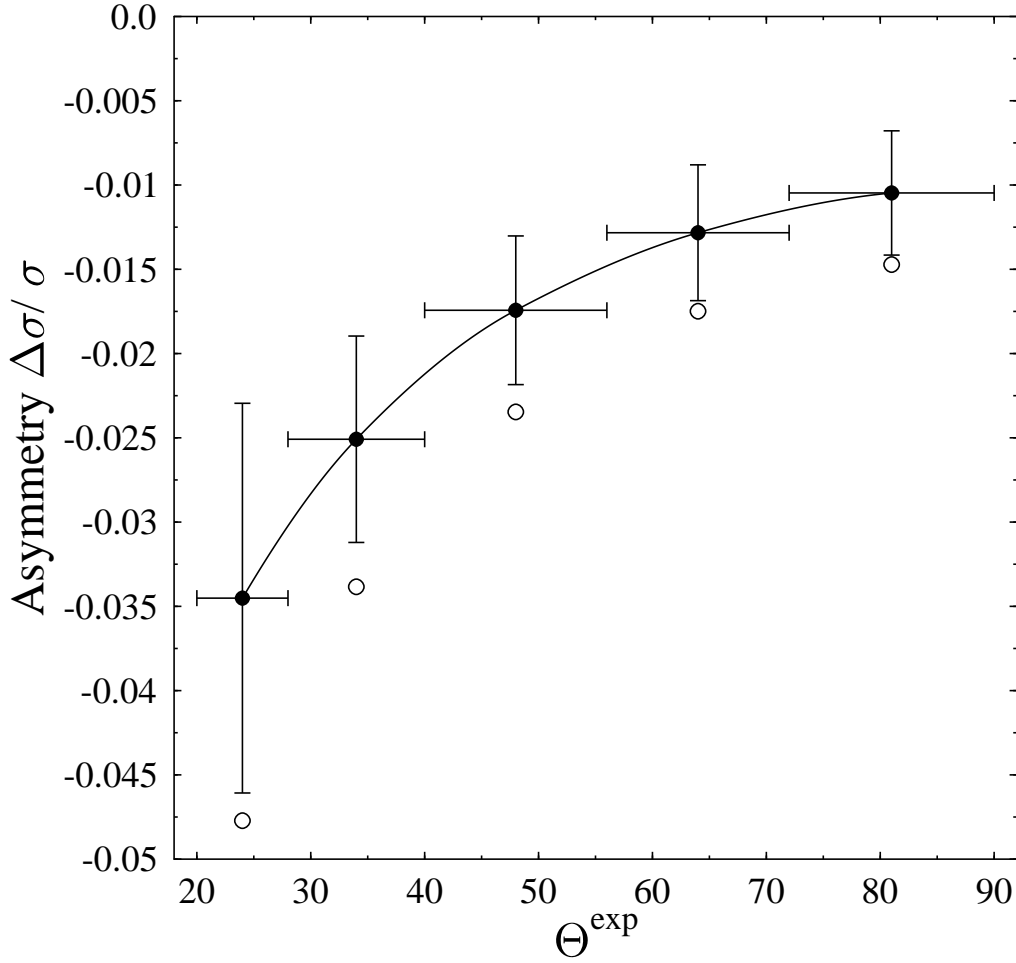


Figure 5: Experimentally accessible asymmetry versus  $\Theta^{\text{exp}}$ . The data are taken from the PEPSI run. The full circles denote the total asymmetry, while the empty circles are the asymmetry if the gluon bremsstrahlung process is switched off. The horizontal bars denote the binning width. In the plot we assumed that proton and electron beam polarizations are 70% each. The error bars show the expected experimental error for  $100 \text{ pb}^{-1}$  per relative polarization.

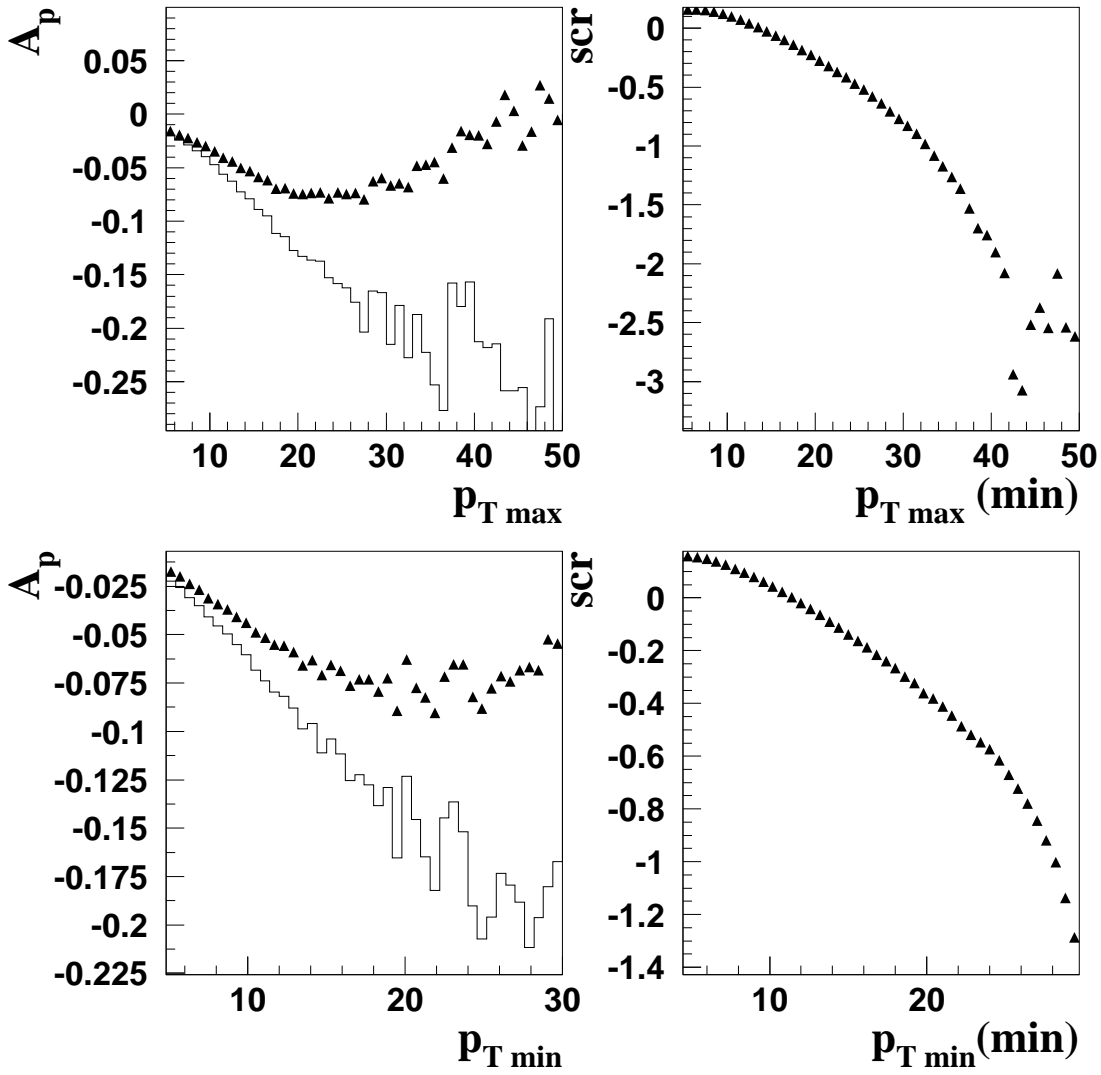


Figure 6: Asymmetry  $A_p$  and reduced significance ( $scr$ ) for the  $p_{T,max}$ - and  $p_{T,min}$  distributions. The histogram on the left hand side shows the asymmetry for photon-gluon fusion only. The triangles show the real asymmetry, where gluon bremsstrahlung together with the photon-gluon fusion is taken into account. The pictures on the right show the significance versus  $p_{T,max}$  and  $p_{T,min}$  lower boundaries. The data are simulated with PEPSI.



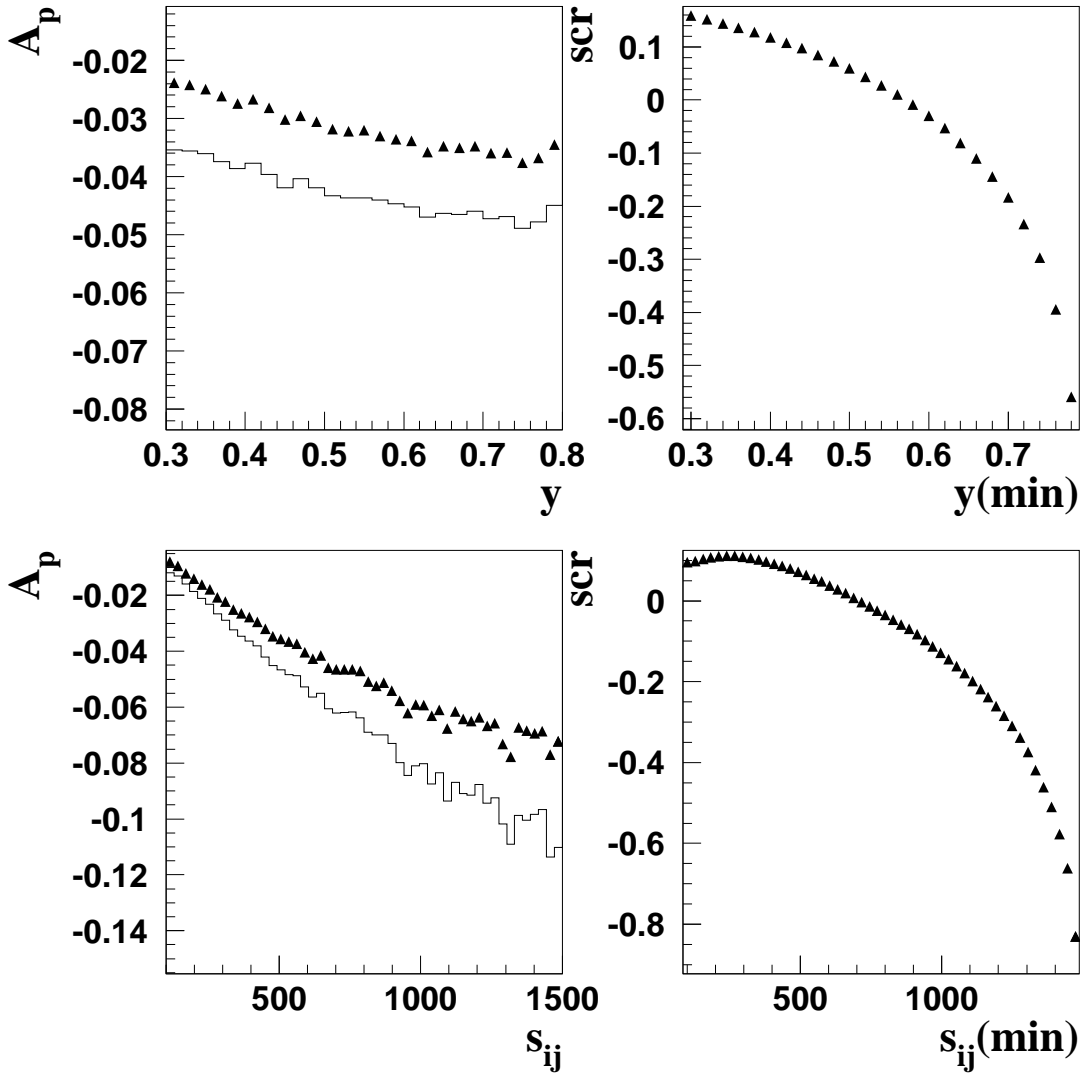


Figure 7: Asymmetry  $A_p$  and reduced significance ( $scr$ ) for the  $y$ - and  $s_{ij}$  distributions. Histogram: no gluon bremsstrahlung; triangles: full asymmetry. Data from PEPSI. The plots on the right show the significance as a function of  $y(\text{min})$  and  $s_{ij}(\text{min})$ , respectively.

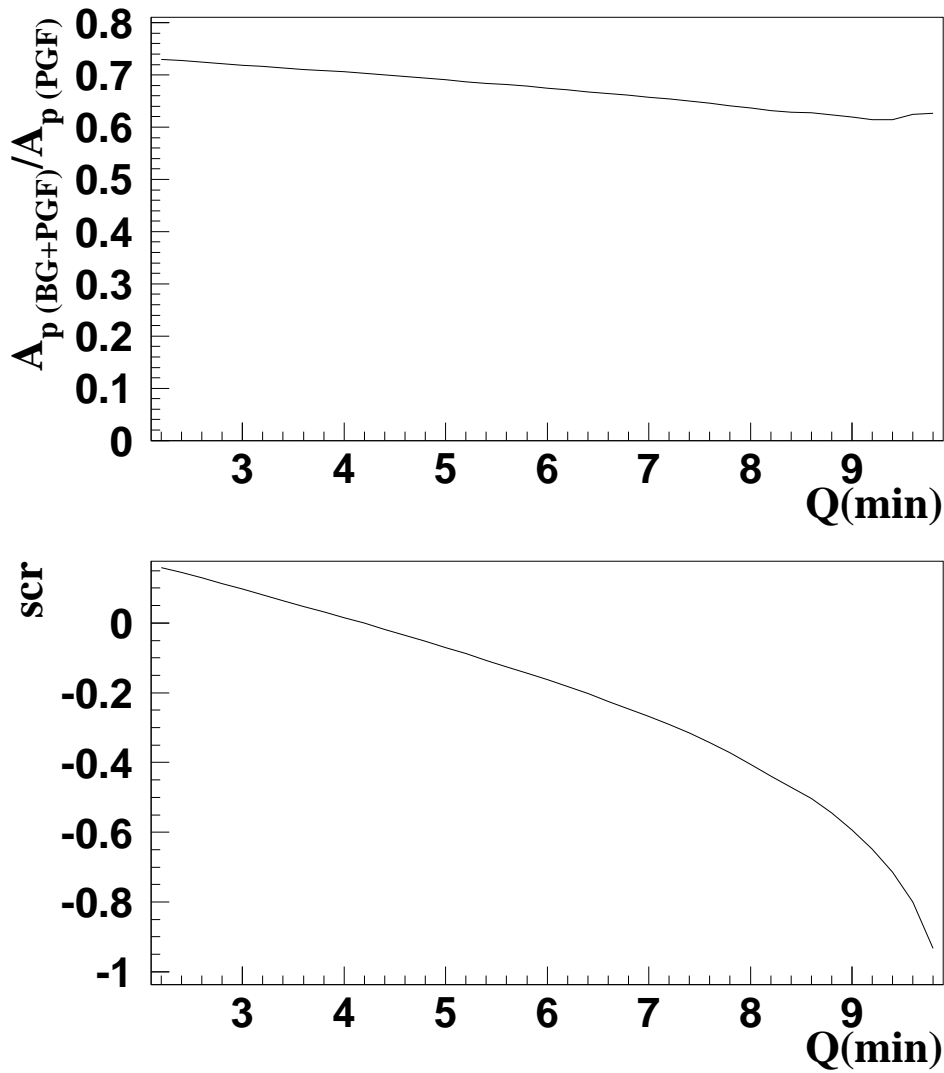


Figure 8: Ratio of the total asymmetry to the pure gluon initiated asymmetry (top) and reduced significance  $scr$  as a functions of  $Q(\text{min})$  (bottom); PEPSI data.